# Development of a real-time 3D laser scanner with wide FOV and an interface using a HMD for teleoperated mobile robots

**FUJIWARA Tomofumi[1], KAMEGAWA Tetsushi[2], and GOFUKU Akio[3]**

*1. Graduate School of Natural Science and Technology, Okayama University, 3-1-1 Tsushimanaka, Kita-ku, Okayama-shi, Okayama, 700-8530, Japan (fujiwara.t@mif.sys.okayama-u.ac.jp)*
*2. Graduate School of Natural Science and Technology, Okayama University, 3-1-1 Tsushimanaka, Kita-ku, Okayama-shi, Okayama, 700-8530, Japan (kamegawa@sys.okayama-u.ac.jp)*
*3. Graduate School of Natural Science and Technology, Okayama University, 3-1-1 Tsushimanaka, Kita-ku, Okayama-shi, Okayama, 700-8530, Japan (fukuchan@sys.okayama-u.ac.jp)*

**Abstract:** We develop a new mechanism for 3D scanning with a Laser Range Finder (LRF) with a wide field of view (FOV) for teleoperated mobile robots. The new mechanism has a function that can change the angle of the tilt of a LRF installed on the mechanism. Therefore the new mechanism can increase and change the FOV in 3D scanning which cannot be done by the other former 3D scanning devices. We also adopt a stereoscopic head mounted display (HMD) which has a wide FOV to show 3D point clouds to operators. This paper explains about our real-time 3D laser scanner and its advantages in a point density and a scanning speed and shows a result of displaying a 3D point cloud on a HMD, Oculus Rift DK1. Displaying results of a wide FOV of real-time 3D scanning show that our system has an ability to be applied for search and rescue activities in disaster areas or inspection and maintenance tasks for nuclear power plants.
**Keyword:** real-time 3D laser scanner; HMD; wide field of view; teleoperation; mobile robot

## 1 Introduction

There is a great demand for mobile robot teleoperation tasks such as search and rescue activities in disaster areas or inspection and maintenance tasks for large-scale and safety critical engineering systems such as nuclear power plants. It is very important for human workers who save victims or maintain power plant facilities to avoid the risk of injury by corruption of buildings and radiation exposures. Therefore, constructing vision sensors and user interfaces for mobile robot teleoperation are the most important issues.

It is very important for a human operator of a teleoperated mobile robot to see visual information from the remote places in order that the human operator can understand the environment. To inspect certain facilities such as nuclear buildings by using a mobile robot, the human operator has to understand the surroundings of the mobile robot. The mobile robot has to have a visual sensor because the human operator cannot see the mobile robot directly. The visual sensor has to be used in bad lighting conditions which are usually unstable in disaster areas, has to provide sense of distance to the human operator, and has to have low communications traffics because communication infrastructures in disaster areas are unreliable. Cameras are mostly implemented in mobile robot teleoperations and are useful, while cameras have disadvantages including that they cannot be used in darkness, they do not provide depth information and they need high communications traffics to send image sequences to the operator. Overhead cameras mounted on the mobile robot can be used for recognizing a relationship between the mobile robot and the obstacles in order that the human operator avoids them. However, overhead cameras usually still have disadvantages in terms of accurate depth perceptions, robustness for darkness and communications traffics. Stereo cameras are useful for the human operator to get depth information of the environment in order to understand the environment more clearly and to avoid obstacles. However, stereo cameras still need higher communications traffics than normal cameras and cannot be used in darkness. Ultrasonic sonars can be used in darkness and can provide depth information, while their accuracy is usually low. On the other hand, laser range finders (LRFs) can get more accurate depth information than ultrasonic sonars, can be used in darkness, and have lower

**Received date: June 2, 2015**
(Revised date: August 11, 2015)

communications traffics than cameras. Therefore, we adopt an LRF as one of visual sensors for mobile robot teleoperations. We assume to use an LRF as a means of supplementing a disadvantage of cameras in the dark conditions in which cameras usually do not work.

Although mobile robot teleoperation has been studied by many researchers for many years, operators' depth perceptions by using 3D point clouds obtained by LRFs have not been addressed sufficiently yet. In fact, robots in preceding studies did not implement depth perception of 3D environmental maps into practice. On the other hand, there are a lot of researches that use stereo cameras and stereoscopic displays to provide operators with depth information [1] such as in robot teleoperation [2, 3], manipulation [4] and military applications [5]. According to a report about more than 150 researches on robot teleoperation [6], stereoscopic displays with a stereo camera are useful in confined and complex space such as the World Trade Center damaged from the terrorist attack [7]. However, the effect of stereoscopic presentation of 3D point clouds obtained by LRFs in such environments has not been clear yet. LRFs can obtain more correct depth information even in darkness compared with stereo cameras. Therefore, LRFs have a potential to improve stereoscopic effects.

We have developed stereoscopic presentation system that displays 3D point clouds to an operator using a stereoscopic display in order to help the operator to teleoperate a mobile robot and to find certain targets in the environment [8, 9]. We have conducted some experiments on finding targets using the system and found that stereoscopic presentation is more useful for finding targets in confined and complex space than in open and flat space. Now we are considering to teleoperate mobile robots in real-time using stereoscopic presentation of 3D point clouds. Therefore, we have to construct a real-time 3D laser scanner because our past research shows that our previous 3D laser scanner performs one cycle of 3D scanning at least in 20 seconds, which is not enough for real-time teleoperations. There are many forms of 3D representation such as surface reconstructions, however, 3D point clouds have an advantage in terms of their computational time, which is important for real-time teleoperations. Therefore, we implement 3D point clouds as a representation method of results of 3D scanning. Presentation methods for real-time 3D point clouds have not been considered well and must be developed. For inspection or search tasks in nuclear facilities or disaster areas, a human operator needs to look around the mobile robot and the facilities such as vertical or horizontal pipe arrangements. Therefore, both a real-time 3D laser scanner with a wider field of view (FOV) and information visualization with a wider FOV are needed.

In this paper, we develop a new mechanism for real-time 3D scanning with a LRF which has a wide FOV. The new mechanism can change the angle of the tilt of a LRF installed on the mechanism in order that it can increase and change the vertical FOV which cannot be done by the other former devices. We also implement a new head mounted display for a wide FOV of real-time 3D point clouds.

## 2 Mobile robot

The mobile robot shown in Fig. 1 is used as a platform in this study. The mobile robot is called a surveyor type robot, which was developed by an R&D project of the New Energy and Industrial Technology Development Organization (NEDO), Japan [10]. The size of the robot is 490(max: 705) x 590 x 400 cubic millimeters and its weight is 24 kilograms. This robot runs at the speed of 1 meter per second at a maximum. It can climb up stairs by extending its flipper arms. The expanded flipper arms are shown on the lower right in Fig. 1.

Mounted sensors on this mobile robot are: a network camera (Axis 213 PTZ) which can be panned and tilted, a wide angle view camera (OPT NM33) on the top of the poll for a following view of the robot, a proximity infrared sensor (SHARP GP2D120) for target detections on the side, the back, the lower and upper front of the robot and a posture tracking sensor (Intersense InertiaCube 3). In particular, this robot has a real-time 3D laser scanner with a wide FOV, which consists of a LRF mounted on a swing mechanism and can perform real-time 3D scanning of the surroundings. This real-time 3D laser scanner is explained in Section 3.

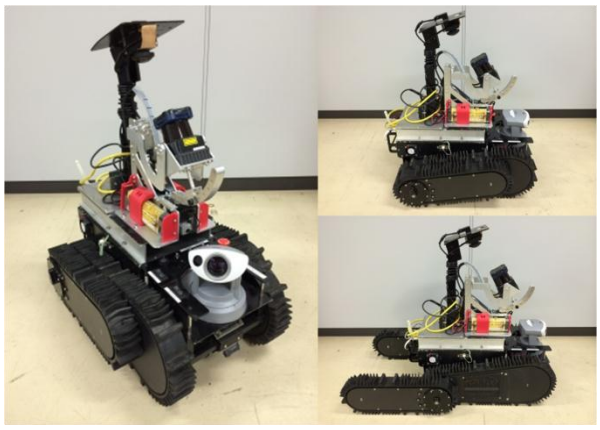

Fig.1 The surveyor type robot with a real-time 3D laser scanner (upper right). Side view in normal locomotion mode (lower right). Side view in extended flippers mode (Left).

# 3 Real-time 3D laser scanner with wide FOV

## 3.1 Requirements for mobile robot teleoperations

We determine requirements for mobile robot teleoperations including a scanning range, accuracy, a vertical FOV, a scanning time, a resolution and a use environment as shown in Table 1. In terms of the scanning time, we first defined that "real-time" is to finish one cycle of 3D scanning in order not to disturb the mobile robot teleoperation. We assume that the mobile robot and an obstacle are approaching each other from the opposite direction. Given that a mobile robot moves at the speed of $v_r$, an obstacle whose size (projected width or height seen from the scanner) is $s_o$ moves at the speed of $v_o$ and a resolution of a LRF is $r_s$, the required cycle of 3D scanning can be derived by

$$T = \frac{d}{v_o + v_r}, \quad (1)$$

where

$$d = s_o / r_s \quad (2)$$

and

$s_o$ [m]: Size (width or height) of obstacle
$v_o$[m/s]: Assumed speed of obstacle
$v_r$[m/s]: Speed of robot
$d$ [m]: Detectable distance
$r_s$[rad]: Resolution of scanner
$T$ [s]: Cycle of 3D scanning

By assuming that $v_r$=0.25[m/s] as a controllable speed, $v_o$=1[m/s] as a human's walking speed, $s_o$=0.2[m] derived by a width of a human leg and $r_s$ =0.025[rad] defined by a LRF (HOKUYO UTM-30LX-EW), we can get $T$=6.4[s]. In this case, the mobile robot can detect the obstacle before crashing by 6.4 seconds cycle of 3D scanning.

The minimum scanning range is defined as 0.1 meters because a mobile robot needs to detect near obstacles appeared in confined and complex space such as damaged buildings or nuclear facilities. The maximum scanning range should be at least 8 meters because we already defined the size of obstacle $s_o$ as 0.2 meters and the resolution of the scanner $r_s$ as 0.025 meters, which derives the detectable distance as 8 meters by Equation (2). The accuracy of scanning should be within $\pm$0.1 meters because a minimum size (width or height) of targets is 0.2 meters. The vertical FOV should be around 180 degrees in order to detect overhead obstacles and obstacles on the ground near the mobile robot. The use environment is both indoor and outdoor because disaster areas or nuclear facilities include both of them.

**Table 1 Specification and requirements for a real-time 3D laser scanner**

| | Specification | Requirement |
|---|---|---|
| Range [m] | 0.1~30 | 0.1~8 or more |
| Accuracy [m] | Max. $\pm$0.05 | < $\pm$0.1 |
| Vertical FOV [deg] | Max. 160 | ≅ 180 |
| Scanning time [s] | 1~ | < 6.4 |
| Resolution [rad] | 0.017~ | < 0.025 |
| Use environment | In and outdoor | In and outdoor |

## 3.2 Development of the scanner

We have developed a new mechanism as shown in Fig. 2 because the former 3D scanning devices do not satisfy the requirements. We have searched for available 3D laser scanners including (a) Velodyne laser scanner, (b) Microsoft Kinect (RGB-D camera), (c) mesa Swiss Ranger (Time of flight camera), and (d) a swing mechanism [11]. However, we have found that they do not satisfy the requirements in Table 1. The device (a) is not able to detect near obstacles in the distance below 1 meter, The devices (b) and (c) have narrow vertical FOVs and can be used for only indoor environments and the devices (a) and (d) have narrow vertical FOVs. In contrast, our developed scanner satisfies all the requirements as shown in Table 1.

Fig.2 Real-time 3D laser scanner which we have developed.

The developed scanner has characteristics below:

1. Equal vertical FOV in all horizontal directions
2. Homogeneous distribution for the density of measurement points
3. Simple control method because of the motor rotation at the constant speed
4. No slip ring which often causes connection troubles, because a LRF itself does not rotate infinitely
5. Adjustable vertical FOV which is able to be adopted for not only inspections in nuclear power plants but also various applications

The definition of constants and variables of the new mechanism is shown in Fig. 3, where

$l_1, l_2$ [m]: Lengths of the blue triangle in Fig. 2

$\alpha$ [rad]: Tilt angle of LRF

$\theta_p$ [rad]: Pitch rotation angle (relative angle between LRF and Link B) indicated by the red arc arrow

$\theta_r$ [rad]: Roll rotation angle (relative angle between Base and Link B) indicated by the red arc arrow

$\theta_m$ [rad]: Motor rotation angle indicated by the red arc arrow

The new mechanism has a function that the vertical FOV can be increased compared with the former swing mechanism [11] which realized a two degree of freedom oscillating movement along pitch and roll axes. The former swing mechanism is driven by only one actuator producing an oscillating movement with a fixed amplitude for the pitch and roll angles. We improved this mechanism in order that the vertical FOV was extended and adjustable. The attached point of Rod in Fig. 3 can be changed along Link A to change the tilt of the LRF from 10 to 80 degrees to expand the vertical FOV. The relationship between the tilt angle $\alpha$ of LRF and the vertical FOV $V$ is expressed by

$$V = 2\alpha. \quad (3)$$

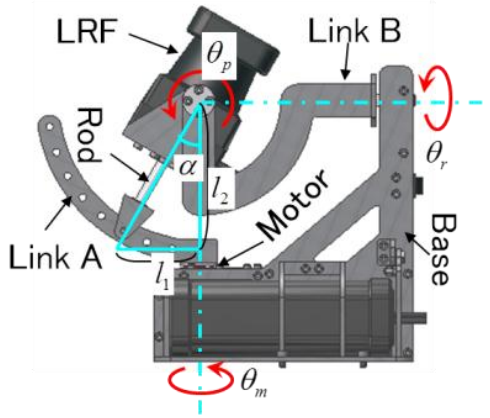


Fig.3 Definition of constants and variables of the developed scanner.

The one cycle of a movement of the developed scanner for 3D scanning is shown in Fig. 4, where $V$=60[deg].

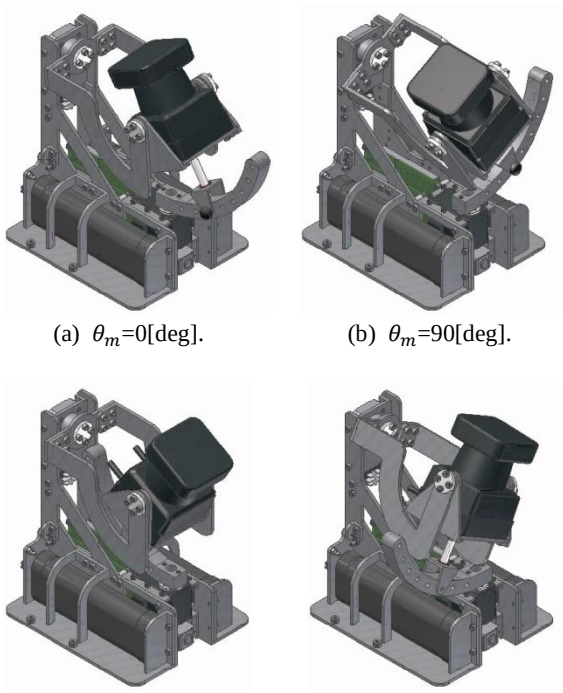

(a) $\theta_m$=0[deg]. (b) $\theta_m$=90[deg].

(c) $\theta_m$=180[deg]. (d) $\theta_m$=270[deg].

Fig.4 Oscillating movement of LRF in one cycle of 3D scanning of the developed scanner in the case of $V$=60[deg].

As shown in Fig. 5, Link B has an arc shape in order to avoid collisions between a laser beam and Link B according to the increasing the vertical FOV. The scanning range of this mechanism can be changed according to the vertical FOV as shown in Fig. 6. The

smaller vertical FOV makes the 3D point clouds denser and the scanned area narrower, and the faster speed of the rotation of the servomotor makes the 3D point clouds sparser. This configuration can be changed according to the environments or tasks.

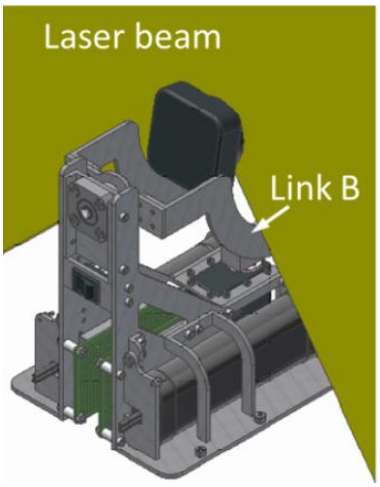


Fig.5 Arc shape of Link B for collision avoidance between the laser beam and Link B of the developed scanner.

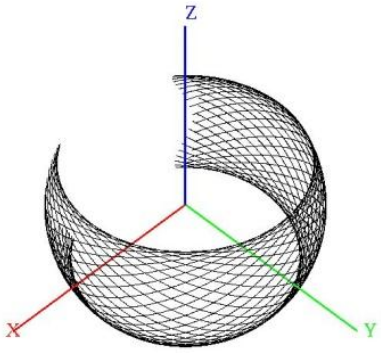


(a) $V$=60[deg].

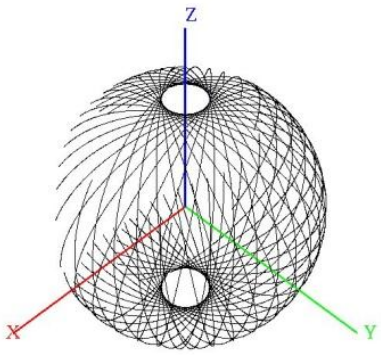


(b) $V$=160[deg].

Fig.6 3D Scanning range of the developed scanner.

The platform performs 3D scans by continuous rotation of a servomotor (ROBOTIS Dynamixel MX-28) to make the scanning plane of a LRF (HOKUYO UTM-30LX-EW) oscillated. This LRF is able to measure 2D distance data with the range up to 30 meters and 270 degrees' angle. The minimum step angle of scanning is 0.25 degrees, thus 1,081 points are measured at one scan. One scan is conducted every 0.025 seconds. The number of obtained points is formulated by

$$n_p = n_{p1} T / t_s \,, \tag{4}$$

where

$n_p$: Number of obtained points at one 3D scan
$n_{p1}$: Number of obtained points at one 2D scan
$t_s$[s]: Scanning cycle of one 2D scan

In this case, we set $n_{p1}$=1,081, $t_s$=0.025[s] and $T$=6.4[s], and get $n_p$=276,736.

### 3.3 Coordinate transformation of 3D point clouds

The measured point clouds are transformed into the world coordinate system by using the roll and pitch rotation angles of the developed scanner and the distance between the mobile robot's coordinate system and the scanner's coordinate system. The roll and pitch rotation angles of the developed scanner are calculated by the motor angle as below. Variables and constants are defined as shown in Fig. 3, where

$$l_1 = l_2 \tan\alpha. \tag{5}$$

Now we can get the roll and pitch rotation angles by

$$\theta_r = \tan^{-1}\left(\frac{l_1 \sin\theta_m}{l_2}\right), \tag{6}$$

$$\theta_p = \tan^{-1}\left(\frac{-l_1 \cos\theta_m}{\sqrt{(l_1 \sin\theta_m)^2 + l_2^2}}\right). \tag{7}$$

Those rotation angles are interpolated to be synchronized with time stamps of laser measurements.

## 4 Performance of the real-time 3D laser scanner

We compare the developed real-time 3D laser scanner with the former swing mechanism [11] to evaluate the performance of the scanner. We conduct two simple experiments which show advantages of our developed scanner. The former swing mechanism has 56 degrees of the vertical FOV. We realize the similar condition to the former swing mechanism by using our developed scanner by setting its vertical FOV as 60 degrees.

### 4.1 Higher point density and higher scanning speed

We obtain 3D point clouds by using the developed real-time 3D laser scanner in the environment as shown in Fig. 7. The results for the former scanner ( $V$ =60[deg]) and our developed scanner ( $V$ =20[deg]) are shown in Fig. 8(a) and (b), respectively. Both results are obtained in 6.3 seconds as one cycle of 3D scanning. Note that black regions show that there is no scanned point and that each point is displayed by grayscale colors according to intensity data which mean how strong reflections of laser beams are detected at the point. Darker colors show weaker intensities.

Fig.7 Experimental environment for comparisons of the point density.

We evaluate point densities in the results for $V$ =60[deg] as the former swing mechanism and $V$=20[deg] as the developed scanner. We count the number of scanned points included in cubes of 0.2 x 0.2 x 0.2 cubic meters whose centers are located at A, B and C as shown in Fig. 8. The result of point densities is expressed as a form of the number of points per 1 cubic meter as shown in Fig. 9. We conduct three trials for each configuration of the scanner and take the average of them. We can see that our developed scanner get much higher point densities for every location than the former swing mechanism. Therefore, our developed scanner is better than the former swing mechanism in terms of point density to display results of 3D scanning. This advantage is helpful when we need higher quality in a 3D point cloud to find certain targets in it during mobile robot teleoperations.

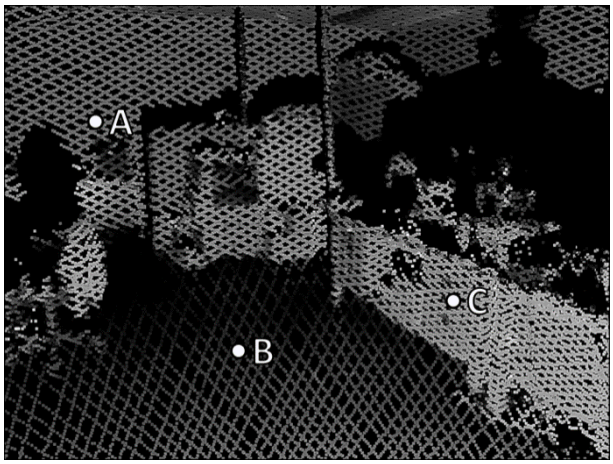


(a) Former scanner ($V$=60[deg], $T$=6.3[s]).


(b) Our developed scanner ($V$=20[deg], $T$=6.3[s]).

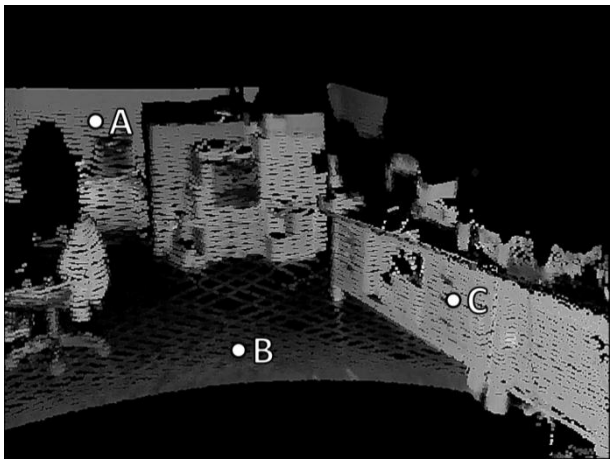


(c) Our developed scanner ($V$=20[deg], $T$=3.1[s]).

Fig.8 Comparison of real-time 3D scanning by changing the vertical FOV and one cycle of 3D scanning. The case (a) indicates the result of the former swing mechanism [11]. The case (b) and (c) indicate the results of our developed real-time 3D scanner. A, B and C indicate where point densities are calculated.

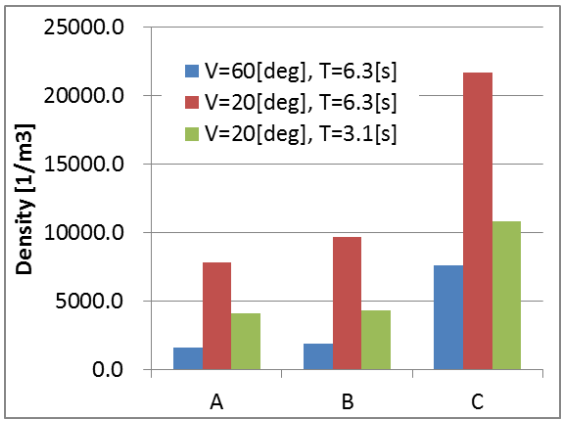


Fig.9 Averaged point densities at A, B and C in Fig. 8. The blue bars indicate the result of the former swing mechanism [11]. The red and green bars indicate the results of our developed real-time 3D scanner.

Furthermore, our developed scanner can increase the scanning speed twice by setting one cycle of 3D scanning as 3.1 seconds when the point density if the case where $V$=60[deg] and $T$=6.3[s] is enough for teleoperation. This result is shown on the bottom in Fig. 8 and its point densities are shown by green bars in Fig. 9. We can see that the point densities in the case of our developed scanner ($V$=20[deg], $T$=3.1[s]) are all higher than those in the case of the former scanner ($V$=60[deg], $T$=6.3[s]). Therefore, our developed system has an advantage on the scanning speed compared with the former swing mechanism.

### 4.2 Wider range of obstacle detections

For mobile robot teleoperation, real-time obstacle detections are important because a mobile robot will stuck or bump and crash on obstacles if it cannot see the obstacles around it in real-time. We conduct 3D scanning in the environment shown in Fig. 10 to show an advantage of the developed scanner on a range of obstacle detections. There are some polls and plates over the mobile robot and a black object on the ground near the mobile robot. We confirm whether the former swing mechanism or our developed scanner detects those obstacles or not. Our developed system can change the vertical FOV from 20 to 160 degrees. Therefore we set $V$=60[deg] as the configuration for the former swing mechanism and $V$=140[deg] for the developed scanner. The both one cycles of 3D scanning are the same, $T$=3.2[s], which was derived by Equations (1) and (2). Here we defined a minimum size of obstacles as $s_o$=0.02[m] by a minimum poll's diameter. The obstacles' speeds are defined as $v_o$=0[m/s] because they were static.

Fig.10 Experimental environment for the range of obstacle detections. There are some polls and plates over the mobile robot and a black object on the ground near the mobile robot.

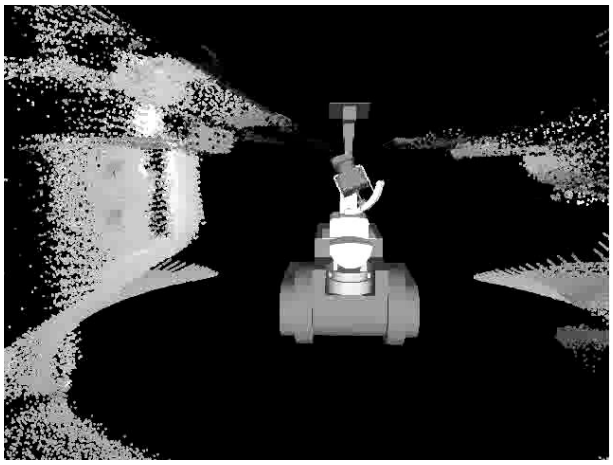

(a) Former scanner ($V$=60[deg], $T$=3.2[s]).

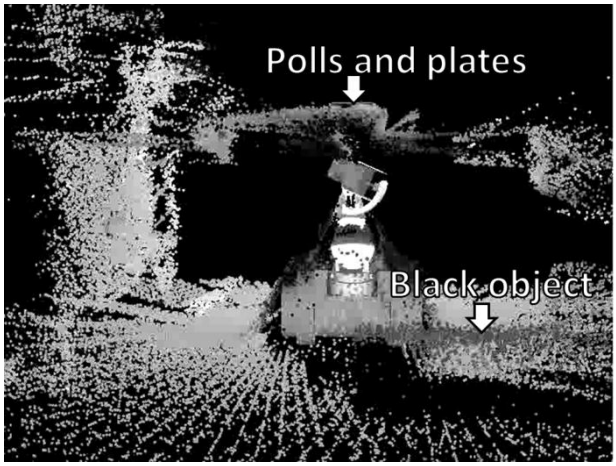


(b) Our developed scanner ($V$=140[deg], $T$=3.2[s]).

Fig.11 Comparison of ranges of obstacle detections. The case (a) indicates the result of the former swing mechanism [11]. The case (b) indicates the result of our developed real-time 3D scanner.

The results are shown in Fig. 11. The former swing mechanism did not detect the polls and plates over the mobile robot as shown in Fig. 11 (a). The former swing mechanism also did not detect the black object on the ground near the mobile robot. Those are because of out of range of the former swing mechanism. Therefore, the mobile robot will crash the obstacles because an operator cannot see them in 3D point clouds. On the other hand, our developed system is able to detect the polls and plates over the mobile robot and the black object on the ground near it as shown in Fig. 11 (b). Therefore, the operator can see the obstacles over and in front of the mobile robot and avoid them in this case. This advantage is helpful for teleoperations in dynamic environments varied by the minute.

## 5 Methods and devices for stereoscopic presentation

There are two main methods of stereoscopic presentation at graphics programs [12]: (1) the off-axis technique that is usually used to create a perception of depth for a human and (2) the toe-in technique that rotates left and right cameras in order to generate azimuth difference and realizes stereoscopic presentation. In this study, the off-axis method is chosen to generate stereo pair images because it is more correct than the toe-in method and is supported by OpenGL.

We adopted a new display device, Oculus Rift DK1, which is one of head mounted displays and has great advantages [13]: (1) a large FOV which improves much immersion in viewing 3D point clouds, (2) sensing of the orientation and the position of the head which prevents motion sickness and improves immersive effects. The other previous HMDs do not have these advantages. Although Oculus Rift is developed for virtual realities and 3D computer games, it also has a potential to be applied to show 3D point clouds and teleoperate mobile robots. While viewing stereo camera images using Oculus Rift requires a mechanism to rotate the camera on a mobile robot to change its view point along the moving of Oculus Rift moved by its user, viewing 3D point clouds do not require it. Therefore changing viewpoint during viewing 3D point clouds with Oculus Rift responds more quickly than viewing video images with stereo cameras because it depends on only the communication between Oculus Rift and a computer and processing powers of the computer which software for displaying 3D point clouds is running. Apparatus of wearing Oculus Rift DK1 is shown in Fig. 12.

Fig.12 Apparatus of wearing Oculus Rift DK1.

## 6 Displaying 3D point clouds on Oculus Rift DK1

A displaying result of 3D point clouds obtained by the developed real-time 3D laser scanner onto Oculus Rift DK1 is shown in Fig. 13. The 3D point clouds are obtained while the mobile robot is teleoperated. The mobile robot in the 3D point cloud is displayed by coordinate frames shown in Fig. 13. We confirmed that the display provided by Oculus Rift had some great advantages such as a large FOV, high immersive effects, no ghost which was sometimes seen on some 3D displays and ability to be able to change a pose of a view point by moving the head without any input devices such as mouse devices. The wide FOV of this display was useful for inspections by looking around the environment while teleoperations. This system has a potential to teleoperate mobile robots for inspections because an operator does not need to switch to a mouse to change a view point and the FOV. On the other hand, we also confirmed that all of visual information from circumstances of an operator was completely shut out by using Oculus Rift, which would not be appreciated by rescue workers. We will also address a motion sickness by experiments with participants in the future by considering many tips not to induce a motion sickness by stereoscopic presentation on literature [14].

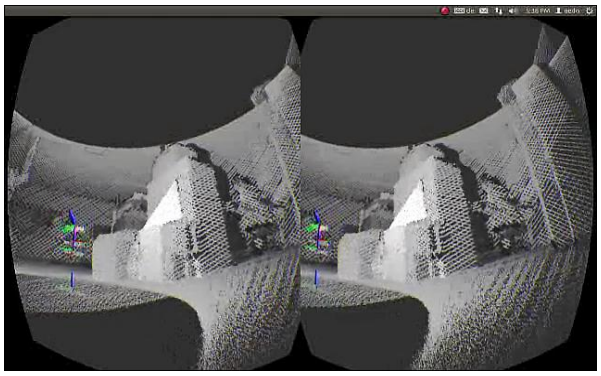

Fig.13 Displaying real-time 3D point clouds on Oculus Rift DK1. The images for left and right eyes are separately displayed according to operator's azimuth difference. Both images are also skewed in order that the operator gets wider FOV of the 3D point clouds through wide angle of lenses.

## 7 Prospects for nuclear facilities

In inspection tasks for nuclear facilities by using teleoperated mobile robots, an operator controls the mobile robot giving attention to the forward ground. The operator also pays attention to obstacles on the both sides of the mobile robot. In the case of inspections of pipe arrangements or tanks largely extended vertically or horizontally, the operator need to take a look around the mobile robot. Therefore, we can adopt our developed 3D laser scanner which can scan the environment on the left, right, top and bottom of the mobile robot in real-time and our developed interface system using Oculus Rift DK1 which can display wider range of 3D point clouds than the former displaying devices.

The requirements for the density and the scanning speed depend on target objects in nuclear facilities. We have already confirmed that our previous 3D laser scanner which cannot perform 3D scanning in real-time was able to scan the environment in the nuclear facility and the results can be useful to estimate shapes and sizes of a facility [15]. On the other hand, those results were still not enough to use for inspection tasks which included narrower and more complicated pipes or equipment. As shown in Fig. 8, the developed scanner can get more detailed 3D point clouds by setting the appropriate vertical FOV and scanning speed. Therefore, the developed scanner can be used for inspection tasks of complicated pipes or equipment. An automatic vertical FOV changing mechanism will be useful.

Color visual information is also useful to teleoperate mobile robots and to inspect nuclear facilities. We assume to use 3D point clouds obtained by our developed scanner mainly to teleoperate a mobile robot in confined and complex environments such as small pipes or polls. We also use 3D point clouds as a rough screening and detection of defects in the facilities. After the rough screening and detection of them, we can use the front camera (Axis 213 PTZ) and the overhead camera (OPT NM33) mounted on the mobile robot to get moving colored images in order to recognize leakages, vibrations and living objects in inspection tasks when the light condition is fine. Our developed system also can combine 3D point clouds from the developed scanner with color images from cameras to colorize the 3D point clouds in order to enhance visual cues for an operator [16].

As a result, our developed system including the mobile robot, the front and overhead cameras, the real-time 3D laser scanner, and the interface system with Oculus Rift can achieve inspection tasks in nuclear power plants.

## 8 Conclusion

We developed the new real-time 3D laser scanner with a wide FOV and adopted Oculus Rift DK1 to display wide FOV of 3D point clouds obtained by a mobile robot in real-time. The developed scanner has advantages in terms of the higher point density, the higher scanning speed and the wider range of obstacle detections compared with the former scanner. As a result, our developed system has a potential to improve teleoperational performance in nuclear facilities for mobile robots. The future work will be to develop a mechanism which can change the vertical FOV automatically according to situations, and to conduct experiments to evaluate this system by participants to apply our system to disaster areas or nuclear power plants.

## Acknowledgement

This research has become possible by support of Professor Dirk Wollherr at Technische Universität München with the Erasmus Mundus EASED support (Grant 2012-5538/004-001) coordinated by CentraleSupélec.

## References


[1] TACHI, S.: Telexistence, World Scientific, 2010.

[2] WATANABE, K., KAWABUCHI, I., KAWAKAMI, N., MAEDA, T., and TACHI, S.T.: Development of a telexistence visual system using a 6-d.o.f. robot head, Advanced Robotics, 2008, 22(10): 1053–1073.

[3] LIVATINO, S., MUSCATO, G., and PRIVITERA, F.: Stereo viewing and virtual reality technologies in mobile robot teleguide, IEEE Transactions on Robotics, 2009, 25(6): 1343–1355.

[4] FERRE, M., ARACIL, R., and NAVAS, M.: Stereoscopic video images for telerobotic applications, Journal of Field Robotics, 2005, 22(3): 131–146.

[5] CHEN, J. Y. C., ODEN, R. V. N., KENNY, C., and MERRITT, J. O.: Evaluation of stereoscopic display for indirect-vision driving and robot teleoperation, The WSTIAC (Weapon Systems Technology Information Analysis Center) Quarterly, 2010, 10(2): 3–9.

[6] CHEN, J. Y. C., HAAS, E. C., and BARNES, M. J.: Human performance issues and user interface design for teleoperated robots, IEEE Transactions on Systems, Man, and Cybernetics, Part C, 2007, 37(6): 1231–1245.

[7] MURPHY, R. R.: Human-robot interaction in rescue robotics, IEEE Transactions on Systems, Man, and Cybernetics, Part C: Applications and Reviews, 2004, 34(2): 138–153.

[8] FUJIWARA, T., KAMEGAWA, T., and GOFUKU, A.: Stereoscopic Presentation of 3D Scan Data Obtained by Mobile Robot. In: Proceedings of the 2011 IEEE International Symposium on Safety, Security and Rescue Robotics (SSRR2011), Kyoto, 2011: 178-183.

[9] FUJIWARA, T., KAMEGAWA, T., GOFUKU, A., and SUGIHARA, T.: Exploration Experiments in Confined and Complex Space by Stereoscopic Presentation of 3D LRF Data (in Japanese). In: Proceedings of 31th annual conference of the Robotics Society of Japan (RSJ2013), Tokyo, 2013: 1J1-05.

[10] KAMEGAWA, T., SATO, N., HATAYAMA, M., UO, Y., and MATSUNO, F.: Design and implementation of grouped rescue robot system using self-deploy networks, Journal of Field Robotics, 2011, 28(6): 977–988.

[11] YOSHIDA, T., IRIE, K., KOYANAGI, E., and TOMONO, M.: Outdoor navigation system using wide view 3d laser scanner and gyro-odometry (in Japanese), Journal of the Society of Instrument and Control Engineers, 2010, 49(9): 608–611.

[12] BOURKE, P., and MORSE, P.: Stereoscopy: Theory and practice. In: Workshop at 13th International Conference on Virtual Systems and Multimedia, 2007.

[13] Oculus VR: http://www.oculus.com/, accessed 18.08.2015.

[14] Oculus VR: Oculus Best Practices, 2015.

[15] FUJIWARA, T., FUKUNAGA, T., KAMEGAWA, T., GOFUKU, A., and MATSUNO, F.: Experiments on Teleoperation and Displaying Environmental Maps by Using an Indoor Searching Robot (in Japanese). In: Proceedings of 55th Joint Automatic Control Conference (JACC2012), Kyoto, 2012: 749-754.

[16] FUJIWARA, T., KAMEGAWA, T., and GOFUKU, A.: Study on Teleoperational Performance for Rescue Robot by Stereoscopic Presentation of 3D Scan Data. In: Proceedings of the first International Symposium on Socially and Technically Symbiotic Systems (STSS2012), Okayama, 2012: 17_1-7.